

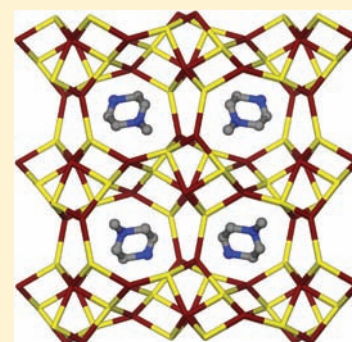
# Divalent-Metal-Stabilized Aluminophosphates Exhibiting a New Zeolite Framework Topology

Lang Shao, Yi Li,\* Jihong Yu,\* and Ruren Xu

State Key Laboratory of Inorganic Synthesis and Preparative Chemistry, College of Chemistry, Jilin University, Changchun 130012, P.R. China

## Supporting Information

**ABSTRACT:** Two divalent-metal-containing aluminophosphates,  $(C_5H_{14}N_2)[Co_2Al_4P_6O_{24}]$  and  $(C_5H_{14}N_2)[Zn_2Al_4P_6O_{24}]$  (denoted as MAPO-CJ62; M = Co, Zn), have been hydrothermally synthesized by using *N*-methylpiperazine as the structure directing agent. Their structures are determined by single crystal X-ray diffraction and further characterized by powder X-ray diffraction, inductively coupled plasma, and thermogravimetric and diffuse reflectance spectroscopy analyses. Both of these two compounds exhibit a new zeolite framework topology. This new zeolite framework contains 1-dimensional 8-ring channels running along the  $[010]$  direction. All the metal and P atoms are tetrahedrally coordinated and alternately connected to each other through bridging O atoms. Inductively coupled plasma analysis shows that the molar ratio of M:Al in MAPO-CJ62 is 1:2. The  $M^{2+}$  ions in MAPO-CJ62 selectively occupy two of the three possible crystallographically distinct positions. A pure aluminophosphate analogue of MAPO-CJ62 without  $M^{2+}$ -incorporation, denoted as AIPO-CJ62, has not been obtained in our experiment so far. The necessity of introducing  $M^{2+}$  ions and their ordered distribution in MAPO-CJ62 has been elucidated by analyzing the distortions of Al-centered tetrahedra in the hypothetical framework of AIPO-CJ62.



## INTRODUCTION

Traditional zeolites are a family of microporous aluminosilicates that are widely used in fields as diverse as catalysis, adsorption, and ion exchange. A typical aluminosilicate zeolite structure contains a three-dimensionally extended crystalline framework with ordered micropores constructed exclusively by  $TO_4$  tetrahedra (T = tetrahedrally coordinated Al or Si atom). In 1982, Wilson and co-workers reported the syntheses of a series of aluminophosphate zeolites for the first time.<sup>1</sup> From then on, many new aluminophosphate-based zeolites have been synthesized.<sup>2–4</sup> Among all the 197 known zeolite framework types, about 60 fall into this category.<sup>5</sup> Aluminophosphate-based zeolites possess pores with openings in various sizes, such as 8-, 10-, 12-, 14-, 18-, and 20-rings. Due to their rich structural varieties, aluminophosphate zeolites have attracted much attention during the past decades.<sup>6</sup>

Generally, the framework of an aluminophosphate zeolite is built from strict alternation of  $PO_4$  and  $AlO_4$  tetrahedra, which ensures the charge neutrality. When  $M^{2+}$  ions (divalent metal ions, such as  $Mg^{2+}$ ,  $Mn^{2+}$ ,  $Zn^{2+}$ , and  $Co^{2+}$ , etc.) are incorporated into aluminophosphate zeolites to substitute a small amount of framework  $Al^{3+}$ , negative charges will be generated around  $M^{2+}$  ions.<sup>7</sup> Besides the traditional properties that porous materials have,  $M^{2+}$ -containing aluminophosphate zeolites may have additional features due to the well-separated active centers. For instance, they could be used as single-site solid catalysts for many reactions.<sup>8–11</sup> In most cases, the  $M^{2+}$  ions substitute the framework  $Al^{3+}$  randomly and could not be distinguished from each other through single crystal structural analysis.

Another important role of  $M^{2+}$ -incorporation is its stabilization effect on distorted zeolite frameworks. In aluminophosphate structures, the Al–O–P angles are close to  $145^\circ$  and only vary in a very short range. In contrast, the M–O–P angles can be much smaller and vary in a wider range of  $120–150^\circ$ . Rigid Al–O–P bonds might cause severe stress and distortions on Al-centered tetrahedra in some aluminophosphate structures. Substitution of rigid distorted Al-centered tetrahedra by more flexible M-centered ones may release the stress and stabilize the whole zeolite framework. Sometimes this stabilization effect is so important that the addition of  $M^{2+}$  ions is necessary to the formation of certain zeolite structures. For example, a number of aluminophosphate zeolites, including ACP-1 (ACO), UCSB-4, UCSB-5, UCSB-6 (SBS), UCSB-8 (SBE), and UCSB-10 (SBT), were synthesized by Stucky and co-workers through addition of  $Co^{2+}$ ,  $Mg^{2+}$ ,  $Zn^{2+}$ , and  $Mn^{2+}$ ;<sup>12–14</sup> the aluminophosphate zeolite MAPO-CJ40 (JRY) with intrinsic framework chirality, was reported by Yu et al. through addition of  $Co^{2+}$  or  $Zn^{2+}$ .<sup>15</sup> In all these examples, target framework structures could only be obtained when  $M^{2+}$  ions were incorporated. The introduction of divalent metal ions has become an effective approach to the synthesis of new zeolite structures.<sup>16</sup>

In this work, we have hydrothermally synthesized two novel divalent-metal-stabilized aluminophosphate zeolites,  $(C_5H_{14}N_2)[Co_2Al_4P_6O_{24}]$  and  $(C_5H_{14}N_2)[Zn_2Al_4P_6O_{24}]$  (de-

Received: July 18, 2011

Published: December 7, 2011

Table 1. Crystal Data and Structure Refinement for MAPO-CJ62

	CoAPO-CJ62	ZnAPO-CJ62
Empirical formula	C <sub>2.50</sub> H <sub>7</sub> Al <sub>2</sub> Co N O <sub>12</sub> P <sub>3</sub>	C <sub>2.50</sub> H <sub>7</sub> Al <sub>2</sub> N O <sub>12</sub> P <sub>3</sub> Zn
Formula weight	448.89	455.33
Temperature	296(2) K	296(2) K
Wavelength	0.71073 Å	0.71073 Å
Crystal system, space group	Orthorhombic, <i>Pbca</i>	Orthorhombic, <i>Pbca</i>
Unit cell dimensions	<i>a</i> = 15.8674(9) Å <i>b</i> = 9.7437(6) Å <i>c</i> = 17.1201(10) Å $\alpha$ = 90° $\beta$ = 90° $\gamma$ = 90°	<i>a</i> = 15.896(3) Å <i>b</i> = 9.7475(19) Å <i>c</i> = 17.070(3) Å $\alpha$ = 90° $\beta$ = 90° $\gamma$ = 90°
Volume	2646.9(3) Å <sup>3</sup>	2644.9(9) Å <sup>3</sup>
Z, Calculated density	8, 2.253 Mg/m <sup>3</sup>	8, 2.287 Mg/m <sup>3</sup>
Absorption coefficient	1.856 mm <sup>-1</sup>	2.417 mm <sup>-1</sup>
<i>F</i> (000)	1784	1808
Crystal size	0.20 × 0.18 × 0.08 mm <sup>3</sup>	0.16 × 0.12 × 0.07 mm <sup>3</sup>
$\theta$ range for data collection	2.38–28.33°	2.39–28.35°
Limiting indices	−14 ≤ <i>h</i> ≤ 21, −13 ≤ <i>k</i> ≤ 12, −21 ≤ <i>l</i> ≤ 22	−21 ≤ <i>h</i> ≤ 21, −13 ≤ <i>k</i> ≤ 7, −22 ≤ <i>l</i> ≤ 22
Reflections collected/unique	18281/3294 [ <i>R</i> <sub>int</sub> = 0.0471]	18221/3292 [ <i>R</i> <sub>int</sub> = 0.0486]
Completeness to $\theta$	28.33, 100.0%	28.35, 99.7%
Refinement method	Full-matrix least-squares on <i>F</i> <sup>2</sup>	Full-matrix least-squares on <i>F</i> <sup>2</sup>
Data/restraints/parameters	3294/6/192	3292/6/192
Goodness-of-fit on <i>F</i> <sup>2</sup>	1.029	1.016
Final <i>R</i> indices [ <i>I</i> > 2 $\sigma$ ( <i>I</i> )]	<i>R</i> <sub>1</sub> = 0.0489, <i>wR</i> <sub>2</sub> = 0.1186	<i>R</i> <sub>1</sub> = 0.0460, <i>wR</i> <sub>2</sub> = 0.1136
<i>R</i> indices (all data)	<i>R</i> <sub>1</sub> = 0.0615, <i>wR</i> <sub>2</sub> = 0.1245	<i>R</i> <sub>1</sub> = 0.0585, <i>wR</i> <sub>2</sub> = 0.1199
Largest diff. peak and hole	1.024 and −0.650 e Å <sup>-3</sup>	0.865 and −0.768 e Å <sup>-3</sup>

noted as MAPO-CJ62; M = Co, Zn), using *N*-methylpiperazine as the structure directing agent. These two structures are isomorphous and exhibit a new zeolite framework topology with one-dimensional 8-ring channels running along the [010] direction. In MAPO-CJ62, M<sup>2+</sup> ions selectively, not randomly, occupy two of the three crystallographically distinct metal positions. In addition, the M<sup>2+</sup>-free aluminophosphate analogue of MAPO-CJ62, denoted as AlPO-CJ62, has not been obtained in our experiment so far. The ordered distribution of M<sup>2+</sup> ions and their important role on the formation of MAPO-CJ62 have been further studied by geometry optimization and distortion analysis on the hypothetical framework of AlPO-CJ62.

## EXPERIMENTAL SECTIONS

**Syntheses of MAPO-CJ62.** The two compounds were prepared under hydrothermal conditions. Typically, Co(OAc)<sub>2</sub>·4H<sub>2</sub>O or Zn(OAc)<sub>2</sub>·2H<sub>2</sub>O, pseudoboehmite (Al<sub>2</sub>O<sub>3</sub>, 62.5%) and 85% H<sub>3</sub>PO<sub>4</sub> were first dispersed into deionized water with stirring for 1 h, followed by addition of *N*-methylpiperazine as the structure directing agent (SDA). The reaction mixture was stirred at room temperature until it was homogeneous, sealed in a 25 mL Teflon-lined stainless steel autoclave, and heated at 180 °C for 3 days. The overall molar ratio of MO:Al<sub>2</sub>O<sub>3</sub>:P<sub>2</sub>O<sub>5</sub>:SDA:H<sub>2</sub>O is 0.33:0.33:1.0:1.0:92. The deep blue crystals of CoAPO-CJ62 and colorless ones of ZnAPO-CJ62 were recovered by sonication and washed with deionized water.

**Characterizations.** The scanning electron microscopy (SEM) images were taken on a JSM-6700F electron microscope operating at 5.0 kV. Powder X-ray diffraction data for MAPO-CJ62 were collected on a Rigaku X-ray diffractometer using Cu K $\alpha$  radiation ( $\lambda$  = 1.5418 Å). Thermogravimetric analysis was performed on a Perkin-Elmer TGA7 unit in air at a heating rate of 10 K min<sup>-1</sup>. Inductively coupled plasma analyses were carried out on a Perkin-Elmer Optima 3300 DV ICP instrument. Elemental analysis was conducted on a Perkin-Elmer 2400 elemental analyzer. UV–visible diffuse reflectance spectroscopy was performed on a Perkin-Elmer UV/vis instrument.

**Structure Determination.** Single crystals of CoAPO-CJ62 with dimensions of 0.20 × 0.18 × 0.08 mm<sup>3</sup> and ZnAPO-CJ62 with dimensions of 0.16 × 0.12 × 0.07 mm<sup>3</sup> were selected for single crystal X-ray diffraction analysis. The data were collected on a Bruker AXS SMART APEX II diffractometer using graphite-monochromated Mo K $\alpha$  radiation ( $\lambda$  = 0.71073 Å) at the temperature of 23 ± 2 °C. Data processing was accomplished using the SAINT processing program.<sup>17</sup> The structures were solved by direct methods and refined on *F*<sup>2</sup> by full-matrix least-squares using the SHELXTL software package.<sup>18</sup> All Co/Zn, Al, P, and O atoms were easily located. There are three crystallographically distinct Al sites. The bond lengths of Al(1)–O and Al(2)–O are significantly longer than those of Al(3)–O, which indicates that M<sup>2+</sup> ions selectively occupy the Al(1) and Al(2) sites rather than Al(3). Inductively coupled plasma analysis shows that the ratio of M:Al is 1:2. Accordingly, the occupancies of M<sup>2+</sup> ions at Al(1) and Al(2) sites were then refined with the constraint on their sum to be unity. The C and N atoms were subsequently located from the difference Fourier maps. Single crystal structure determination shows that the *N*-methylpiperazine molecules are positionally disordered, and their diprotonation is suggested by charge balance. All non-H atoms were refined anisotropically. The structure details are given in Table 1.

## RESULTS AND DISCUSSION

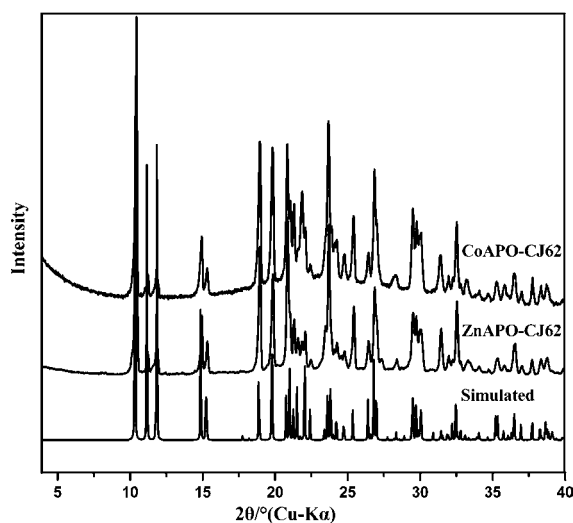
**Syntheses and Characterizations of MAPO-CJ62.** Pure phases of MAPO-CJ62 could be prepared in the reaction system of 0.33 MO/0.33 Al<sub>2</sub>O<sub>3</sub>/1.0 P<sub>2</sub>O<sub>5</sub>/1.0 *N*-methylpiperazine/92 H<sub>2</sub>O at 180 °C for 3 days. There are several factors affecting the syntheses of MAPO-CJ62. When the molar ratio of MO/Al<sub>2</sub>O<sub>3</sub> in the reaction mixture was below 0.75 or above 1.25, a dense phase was formed instead of MAPO-CJ62. The pH value also had great influence on the formation of MAPO-CJ62. The best pH value for the syntheses of MAPO-CJ62 was in the range of 4 to 5. As shown in Table 2, lower pH value might induce the formation of berlinite, while higher pH value gave the formation of MAPO-CHA.<sup>5</sup> The usage of water as the

**Table 2.** Synthetic Conditions and Resulting Products (M = Co or Zn, SDA= *N*-methylpiperazine)

No.	MO	Al <sub>2</sub> O <sub>3</sub>	P <sub>2</sub> O <sub>5</sub>	SDA	resulting products	pH value
1	0.33CoO	0.33	1	0.75	berlinite crystal	4.24
2	0.33CoO	0.33	1	1	CoAPO-CJ62	4.65
3	0.33CoO	0.33	1	1.5	CoAPO-CJ62 and CoAPO-CHA	5.36
4	0.33CoO	0.33	1	1.75	CoAPO-CHA	5.71
5	0.33CoO	0.33	1.5	1.25	berlinite crystal	4.2
6	0.33CoO	0.33	1.5	1.5	CoAPO-CJ62	4.57
7	0.33CoO	0.33	1.5	1.75	CoAPO-CJ62 and CoAPO-CHA	4.9
8	0.33CoO	0.33	1.5	2	CoAPO-CHA	5.31
9	0.33CoO	0.33	2	2.5	berlinite crystal	3.94
10	0.33CoO	0.33	2	3.5	CoAPO-CJ62 and CoAPO-CHA	5.25
11	0.33CoO	0.33	2	4	CoAPO-CHA	5.84
12	0.33ZnO	0.33	1	0.75	ZnAPO-CJ62	3.84
13	0.33ZnO	0.33	1	1	ZnAPO-CJ62 and ZnAPO-CHA	4.49
14	0.33ZnO	0.33	1.5	1.5	ZnAPO-CJ62 and ZnAPO-CHA	4.47
15	0.33ZnO	0.33	1.5	1.75	ZnAPO-CJ62 and ZnAPO-CHA	4.91

solvent was also very important to the formation of MAPO-CJ62. When ethylene glycol, tetraethylene glycol, or triethylene glycol was used as the solvent, no MAPO-CJ62 was formed. When fluorine ions were used instead of divalent metal ions, only a layered aluminophosphate  $[(C_4H_{12}N_2)[Al_2(PO_4)_2(H_2O)_2F_2]]^{19}$  was obtained. Pure aluminophosphate AlPO-CJ62 without  $M^{2+}$ -incorporation has not been obtained in our experiment so far, indicating that the divalent metal ions play an important role in the formation of MAPO-CJ62.

The as-prepared crystals of MAPO-CJ62 are both parallelepiped-like, as shown in the SEM images in Supporting Information Figure S1. The experimental powder X-ray diffraction patterns of MAPO-CJ62 and the simulated one calculated from the crystal structure of CoAPO-CJ62 are shown in Figure 1. They are in good agreement with each other, confirming the phase purity of the as-synthesized products.

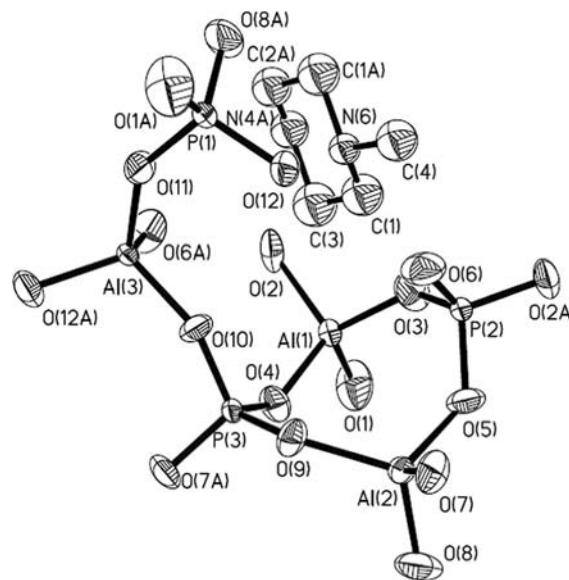
**Figure 1.** Experimental and simulated X-ray diffraction patterns of MAPO-CJ62.

Elemental analysis, as presented in Supporting Information Table S1, shows the molar ratio of M:Al:P to be 1:2:3. The compositional analysis results are in agreement with the empirical formula, that is,  $(C_5H_{14}N_2)[M_2Al_4P_6O_{24}]$ , given by single crystal structure analysis.

The thermogravimetric curves of MAPO-CJ62 were measured in the temperature range of 25 to 800 °C (Supporting Information Figure S2). The weight losses between 50 and 200 °C correspond to the removal of the physically adsorbed water molecules, and the weight losses of 10.51% for CoAPO-CJ62 (calcd. 11.36%) and 10.60% for ZnAPO-CJ62 (calcd. 11.20%) between 200 and 800 °C correspond to the gradual decomposition and release of diprotonated *N*-methylpiperazine molecules in the structures. The powder X-ray diffraction analysis shows that the framework of MAPO-CJ62 transformed into MAPO-tridymite upon calcination at 550 °C.

The valence state and the coordination state of Co ions in CoAPO-CJ62 were confirmed by UV–visible diffuse reflectance spectroscopy, as shown in Supporting Information Figure S3. There are three peaks at 536, 582, and 630 nm, which are characteristic for tetrahedrally coordinated  $Co^{2+}$  ions.<sup>20</sup>

**Structure Description.** CoAPO-CJ62 crystallizes in the orthorhombic space group *Pbca* (No. 61). The structure of CoAPO-CJ62 contains a three-dimensional anionic  $[Co_2Al_4P_6O_{24}]^{2-}$  framework constructed from strict alternation of  $AlO_4/CoO_4$  tetrahedra and  $PO_4$  tetrahedra. As shown in Figure 2, there are three crystallographically distinct P sites and

**Figure 2.** Thermal ellipsoids of CoAPO-CJ62 given at 50% probability, showing the atomic labeling scheme. Al(1) and Al(2) sites are both occupied by  $Co^{2+}$  ions and  $Al^{3+}$  ions.

three Al sites in the framework. The P–O bond distances are in the range between 1.489(4) and 1.530(3) Å (Supporting Information Table S2), which are in good agreement with the typical P–O bond distances in other reported aluminophosphate structures. The average bond distances of Al(1)–O and Al(2)–O are 1.847 and 1.815 Å (Supporting Information Table S2), which lie between the typical bond lengths of Al–O (1.73 Å) and Co–O (1.94 Å). This implies that the Al(1) and Al(2) sites are co-occupied by  $Al^{3+}$  and  $Co^{2+}$  ions.<sup>12</sup> Single crystal data and elemental analysis suggest that the occupancies of



Co<sup>2+</sup> ions at Al(1) and Al(2) sites are both about 50%. The average bond length of Al(3)–O is 1.733 Å (Supporting Information Table S2), indicating that the Al(3) sites are occupied solely by Al<sup>3+</sup> ions. The symmetry, framework structure, bond distances, and site occupancies of ZnAPO-CJ62 are very similar to those of CoAPO-CJ62, which can be found in Table 1 and Supporting Information Table S3.

The framework of MAPO-CJ62 possesses 1-dimensional 8-ring channels running along the [010] direction (Figure 3a).

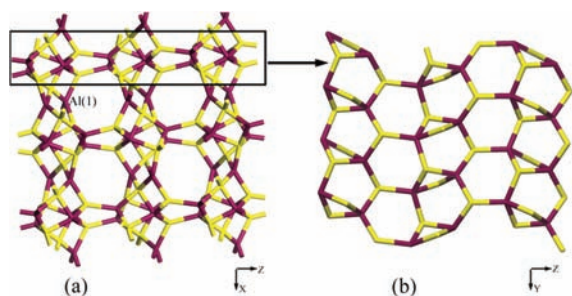


**Figure 3.** (a) Framework of MAPO-CJ62 viewed along the [010] direction. (b) The 2-dimensional (4,6) net. (purple: Al/M, yellow: P).

The free diameters of the 8-ring channels are  $2.5 \times 4.3 \text{ \AA}^2$  (calculated from the atomic coordinates and van der Waals diameters of oxygen atoms). The framework density of MAPO-CJ62 is 18.1 T/1000 Å<sup>3</sup>. As shown in Figure 3b, the framework of MAPO-CJ62 contains 2-dimensional (4,6) nets stacked along the [100] direction. Such (4,6) nets have been reported in several layered aluminophosphates<sup>21</sup> with stoichiometry of Al<sub>2</sub>P<sub>3</sub>O<sub>12</sub><sup>3-</sup>. These layered (4,6) nets are connected together through the Al(1) sites to form a 3-periodic net which exhibits a new zeolite topology. The vertex symbols of MAPO-CJ62 are listed in Supporting Information Table S4. As shown in Figure

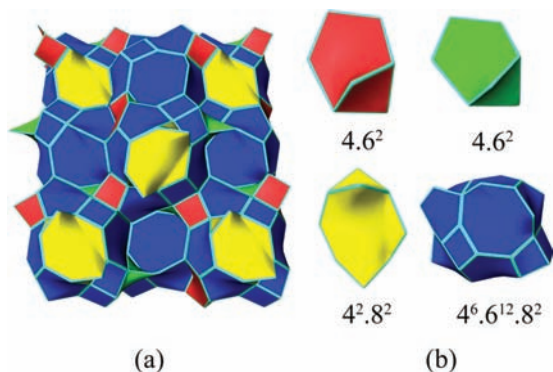


**Figure 4.** (a) Framework of MAPO-CJ62 displayed by tiling. (b) The tiles with the face symbols of [4.6<sup>2</sup>], [4.6<sup>2</sup>], [4<sup>2</sup>.8<sup>2</sup>], and [4<sup>6</sup>.6<sup>12</sup>.8<sup>2</sup>].

4a, this new 3-periodic net is carried by a unique natural tiling with a transitivity of (6 12 9 4).<sup>22</sup> There are four nonequivalent 3-dimensional tiles in this tiling, two of them have the same face symbols of [4.6<sup>2</sup>], one of [4<sup>2</sup>.8<sup>2</sup>], and one of [4<sup>6</sup>.6<sup>12</sup>.8<sup>2</sup>], respectively (Figure 4b). The [4.6<sup>2</sup>] and [4<sup>2</sup>.8<sup>2</sup>] tiles are frequently observed in other aluminophosphate zeolites, such as AEN, AFN, ANA, and JRY; however, the [4<sup>6</sup>.6<sup>12</sup>.8<sup>2</sup>] tile in MAPO-CJ62 is a new tile which has not been observed in any previously reported zeolite structures. Disordered diprotonated *N*-methylpiperazine molecules are located inside these new tiles

to balance the negative charges in the framework (Supporting Information Figure S4).

**Distortion Analysis.** Bond distance analysis shows that M<sup>2+</sup> ions selectively occupy two of the three possible Al sites. In addition, divalent-metal-free AlPO-CJ62 could not be obtained in experiment when M<sup>2+</sup> ions were not introduced into reaction mixtures. These facts imply that M<sup>2+</sup> ions are crucial to the formation of MAPO-CJ62. To understand these phenomena, a hypothetical structure model of M<sup>2+</sup>-free AlPO-CJ62 was built by replacing all the M<sup>2+</sup> ions in MAPO-CJ62 by Al<sup>3+</sup> ions. The framework geometry of AlPO-CJ62 was further optimized using the GULP code<sup>23</sup> based on shell-model ion pair potentials developed by Gale and Henson.<sup>24</sup> In the optimized structure model, two types of Al-centered tetrahedra were considered. One type of tetrahedra are composed of the central Al ions and their coordinated O atoms, denoted as AlO<sub>4</sub>; the others are composed of the central Al ions and the four nearest P atoms, denoted as AlP<sub>4</sub> (Figure 5). In an ideal tetrahedron, all

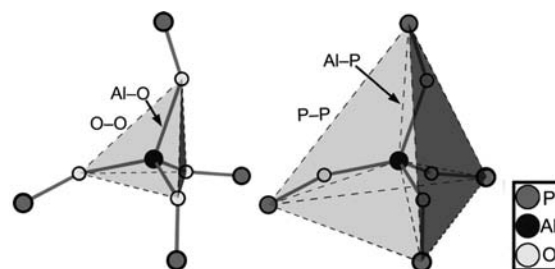


**Figure 5.** Two types of tetrahedra in hypothetical framework of AlPO-CJ62: AlO<sub>4</sub> (left) and AlP<sub>4</sub> (right). The edges considered in distortion analysis are labeled.

equivalent edges should have equal lengths. Any distortion from the ideal shape would introduce additional stress on the tetrahedron and make the whole framework structure unstable.<sup>15</sup> The distortions in existing structures are usually very tiny and negligible; on the contrary, the structures with severe distortions might not be stable enough to be synthesized in reality. Hence, the tetrahedral distortion degree would be a useful tool to predict the stability and feasibility of a hypothetical 4-connected framework structure. One of the simplest methods to measure the distortion degree is to calculate the standard deviation ( $\sigma$ ) of edges in a tetrahedron (Figure 5). The standard deviation of edges in an ideal tetrahedron would be 0, and slightly larger than 0 in existing structures. As shown in Table 3, for both of the AlO<sub>4</sub> and AlP<sub>4</sub> tetrahedra, the standard deviations of edges in Al(1)- and

**Table 3. Distortion Analysis for the Hypothetical Framework of AlPO-CJ62<sup>a</sup>**

	AlO <sub>4</sub>			AlP <sub>4</sub>		
	$\sigma_{\text{Al-O}}$ (Å)	$\sigma_{\text{O-O}}$ (Å)	CShM (%)	$\sigma_{\text{Al-P}}$ (Å)	$\sigma_{\text{P-P}}$ (Å)	CShM (%)
Al(1)	0.0142	0.0803	0.290	0.0413	0.603	6.86
Al(2)	0.0216	0.0550	0.135	0.0552	0.601	5.38
Al(3)	0.00391	0.0346	0.0460	0.0166	0.466	2.52

<sup>a</sup> $\sigma$ : standard deviation. CShM: continuous shape measure. CShM calculates the deviation of a polyhedron from its ideal shape and scales the deviation into the interval from 0% to 100%. The CShM value of an ideal tetrahedron would be 0% and the most distorted would be 100%.

Al(2)-centered tetrahedra are much larger than those of Al(3)-centered tetrahedra. This implies that Al(1)- and Al(2)-centered tetrahedra are much more distorted than Al(3)-centered tetrahedra in the hypothetical framework of  $M^{2+}$ -free AlPO-CJ62. In addition, a more sophisticated method to calculate the polyhedron distortions, i.e., continuous shape measure (CShM),<sup>25</sup> was performed using the SHAPE tool.<sup>26</sup> The CShM values for each type of tetrahedra in AlPO-CJ62 are also shown in Table 3. Similar to the standard deviation values of edges, CShM results also show that the Al(1)- and Al(2)-centered tetrahedra are much more distorted than Al(3)-centered tetrahedra. Since M-centered tetrahedra are more flexible than Al-centered ones, introducing  $M^{2+}$  ions to substitute the  $Al^{3+}$  ions at Al(1) and Al(2) sites would release the stress generated from distortions and further stabilize the whole framework structure. This might be the reason  $M^{2+}$  ions selectively occupy Al(1) and Al(2) sites in MAPO-CJ62 and  $M^{2+}$ -free AlPO-CJ62 is difficult to obtain in experiment.

## CONCLUSIONS

Novel divalent-metal-stabilized aluminophosphate zeolites MAPO-CJ62 have been hydrothermally synthesized by using *N*-methylpiperazine as the structure directing agent. MAPO-CJ62 exhibits a new zeolite framework type with 1-dimensional 8-ring channels running along the [010] direction. The ratio of M:Al in MAPO-CJ62 is 1:2. Different from their random distribution in most other aluminophosphate zeolites,  $M^{2+}$  ions selectively occupy two of the three possible Al sites, i.e., Al(1) and Al(2) sites. In addition, pure aluminophosphate AlPO-CJ62 could not be obtained in experiment. Structural optimization and distortion analysis reveal that serious distortions exist in Al(1)- and Al(2)-centered tetrahedra in the hypothetical framework of AlPO-CJ62. To release the stress generated in these two sites, incorporation of  $M^{2+}$  ions appears necessary to form flexible M-centered tetrahedra instead of rigid Al-centered tetrahedra. Thus, the introduction of divalent metal ions becomes a favorable factor for the formation of the framework of MAPO-CJ62. Our results prove once again that divalent metal ions have considerable stabilization effect on distorted zeolite frameworks and would be a useful tool in pursuit of novel zeolite structures.

## ASSOCIATED CONTENT

### Supporting Information

The compositional analysis results for MAPO-CJ62, the crystallographic information files (CIF) of MAPO-CJ62, SEM images of MAPO-CJ62, the vertex symbols of MAPO-CJ62, the thermogravimetric curves of MAPO-CJ62, the UV-visible diffuse reflectance spectroscopy of CoAPO-CJ62, selected bond lengths and angles for MAPO-CJ62. This material is available free of charge via the Internet at <http://pubs.acs.org>.

## AUTHOR INFORMATION

### Corresponding Author

\*E-mail: [yili@jlu.edu.cn](mailto:yili@jlu.edu.cn) (Y.L.); [jihong@jlu.edu.cn](mailto:jihong@jlu.edu.cn) (J.Y.).

## ACKNOWLEDGMENTS

This work is supported by the National Natural Science Foundation of China and the State Basic Research Project of China (Grant: 2011CB808703).

## REFERENCES

- (1) Wilson, S. T.; Lok, B. M.; Messina, C. A.; Cannan, T. R.; Flanigen, E. M. *J. Am. Chem. Soc.* **1982**, *104*, 1146–1147.
- (2) Bennett, J. M.; Cohen, J. P.; Flanigen, E. M.; Pluth, J. J.; Smith, J. V. *ACS Symp. Ser.* **1983**, *218*, 109–118.
- (3) Davis, M. E.; Saldarriaga, C.; Montes, C.; Garces, J.; Crowder, C. *Nature* **1988**, *331*, 698–699.
- (4) Li, Y.; Yu, J.; Xu, R. AlPO Database: <http://mezeopor.jlu.edu.cn/alpo/>.
- (5) Baerlocher, Ch.; McCusker, L. B. Database of Zeolite Structures: <http://www.iza-structure.org/databases/>.
- (6) Yu, J.; Xu, R. *Chem. Soc. Rev.* **2006**, *35*, 593–604.
- (7) Hartmann, M.; Kevan, L. *Res. Chem. Intermed.* **2002**, *28*, 625–695.
- (8) Thomas, J. M.; Raja, R. *Acc. Chem. Res.* **2008**, *41*, 708–720.
- (9) Hartmann, M.; Kevan, L. *Chem. Rev.* **1999**, *99*, 635–663.
- (10) Thomas, J. M.; Raja, R. *Microporous Mesoporous Mater.* **2007**, *105*, 5–9.
- (11) Thomas, J. M.; Raja, R.; Lewis, D. W. *Angew. Chem., Int. Ed.* **2005**, *44*, 6456–6482.
- (12) Feng, P.; Bu, X.; Stucky, G. D. *Nature* **1997**, *388*, 735–741.
- (13) Bu, X.; Feng, P.; Stucky, G. D. *Science* **1997**, *278*, 2080–2085.
- (14) Bu, X.; Feng, P.; Gier, T. E.; Stucky, G. D. *Microporous Mesoporous Mater.* **1998**, *25*, 109–117.
- (15) Song, X.; Li, Y.; Gan, L.; Wang, Z.; Yu, J.; Xu, R. *Angew. Chem., Int. Ed.* **2009**, *48*, 314–317.
- (16) Čejka, J.; Corma, A.; Zones, S. I. *Zeolites and Catalysis: Synthesis, Reactions and Applications*; WILEY-VCH Verlag GmbH & Co. KGaA: Weinheim, 2010.
- (17) SAINT; Bruker AXS Inc., 5465 East Cheryl Parkway, Madison, WI 53711–5373, USA, 2000.
- (18) SHELXTL; Bruker AXS Inc., 5465 East Cheryl Parkway, Madison, WI 53711–5373, USA, 2000.
- (19) Wang, M.; Li, J.; Li, Y.; Song, X.; Yu, J.; Xu, R. *Chem. J. Chin. Univ.* **2005**, *26*, 1027–1029.
- (20) Verberckmoes, A. A.; Weckhuysen, B. M.; Schoonheydt, R. A. *Microporous Mesoporous Mater.* **1998**, *22*, 165–178.
- (21) (a) Oliver, S.; Kuperman, A.; Lough, A.; Ozin, G. A. *Chem. Mater.* **1996**, *8*, 2391–2398. (b) Oliver, S.; Kuperman, A.; Lough, A.; Ozin, G. A. *Chem. Commun.* **1996**, 1761–1762.
- (22) Blatov, V. A.; Delgado-Friedrichs, O.; O’Keeffe, M.; Proserpio, D. M. *Acta Crystallogr.* **2007**, *A63*, 418–425.
- (23) Gale, J. D.; Rohl, A. L. *Mol. Simul.* **2003**, *29*, 291–341.
- (24) Gale, J. D.; Henson, N. J. *J. Chem. Soc., Faraday Trans.* **1994**, *90*, 3175–3179.
- (25) Pinsky, M.; Avnir, D. *Inorg. Chem.* **1998**, *37*, 5575–5582.
- (26) Continuous Symmetry Measures, <http://www.csm.huji.ac.il/new/>.